

## Comparison of molecular structure and selected physicochemical properties of spelt wheat and common wheat starches

EWELINA NOWAK – LIDIA KRZEMINSKA-FIEDOROWICZ –  
GOHAR KHACHATRYAN – MACIEJ FIEDOROWICZ

### Summary

Molecular weight ( $M_w$ ) and radii of gyration ( $R_g$ ) of starch polysaccharide chains, distribution of amylopectin structural units, crystallinity, thermal properties, pasting viscosity profiles, susceptibility to  $\alpha$ -amylolysis, swelling power and solubility of spelt and wheat starches isolated from commercially available spelt and wheat flours were studied. Average molecular weight  $M_w$  of polysaccharide chains eluted under the whole complex peak from high-performance size exclusion chromatography (HPSEC) column was found to be  $0.829 \times 10^7$  g·mol<sup>-1</sup> for spelt starch and  $2.307 \times 10^7$  g·mol<sup>-1</sup> for wheat starch. Significant differences in amylopectin chain length distribution between spelt and wheat starch were found. Shortest A type chains with  $M_w = 3.418 \times 10^3$  g·mol<sup>-1</sup> and  $R_g = 65.4$  nm constituted 88.2% of total mass of debranched spelt starch, whereas mass ratio of respective chains of wheat starch with  $M_w = 5.277 \times 10^3$  g·mol<sup>-1</sup> and  $R_g = 88.2$  nm was found to be 32.7%. Wheat starch was more susceptible to  $\alpha$ -amylolysis than spelt starch. Enzymatic hydrolysis, rate constant for the first stage of hydrolysis ( $k_1 = 4.5 \times 10^{-3}$  mg·ml<sup>-1</sup>·min<sup>-1</sup>) and final hydrolysis extent (42.5%) for wheat starch were significantly higher than the respective values for spelt starch ( $k_1 = 2.3 \times 10^{-3}$  mg·ml<sup>-1</sup>·min<sup>-1</sup>; 35%).

### Keywords

amylopectin; molecular weight; polysaccharides; spelt

Spelt (*Triticum spelta*) is a hexaploid species of wheat (*Triticum*). Spelt is an ancient grain that traces its heritage back long before many wheat hybrids. It was widely cultivated in Europe since bronze age up to medieval times. Nowadays, spelt is cultivated only in limited regions (Eastern Europe and Spain mainly) where environmental conditions prevent cultivation of wheat. However in the last years, growing interest in the use of spelt is observed. Spelt could be cultivated without the application of fertilizers and is very resistant to frosts [1] and to the crop diseases [2], therefore grows quite successfully without the application of herbicides, pesticides or fungicides. Additionally, it offers a broader spectrum of nutrients compared to many of its more inbred cousins in the *Triticum* family.

Previous reports indicated that wild and primitive wheat species, such as *Triticum monococum*, *Triticum dicoccon* or *Triticum dicocoides*, were

found to accumulate in grain higher micronutrient levels than those in cultivated wheat and advanced lines [3–5]. Recently, GOMEZ-BECERRA et al. [6] studied grain contents of protein and mineral nutrients in large number of spelt wheat genotypes, identifying several spelt genotypes exhibiting very high grain contents of protein and microelements, especially Zn and Fe.

Starch is a main component of the endosperm and starch molecular structure determines functional properties of the end-use products. In wheat kernel, starch constitutes 63–72% of total mass [7]. Starch consists of two polysaccharides, namely, amylopectin and amylose. Amylose is a component with smaller molecular weight and an essentially linear  $\alpha$ -1,4-glucan molecule, which contains only tiny amounts of  $\alpha$ -1,6-branch linkages. Amylopectin is a component with much higher molecular weight and a branched  $\alpha$ -1,4- and  $\alpha$ -1,6-glucan. Side chains of amylopectin

---

Ewelina Nowak, Lidia Krzeminska-Fiedorowicz, Gohar Khachatryan, Maciej Fiedorowicz, Department of Chemistry and Physics, University of Agriculture, 122 Balicka Str., 30-149 Cracow, Poland.

Correspondence author:

Maciej Fiedorowicz, tel: 48126624139, fax: 48126634336, e-mail: rrfiedor@cyf-kr.edu.pl

molecule form left stranded double helix [8]. The functional properties of starch granules are affected by many factors e.g. amylose [9], lipid and phospholipid [10, 11] content, starch granule size distribution, crystalline structure and granule structure [12]. According to the widely accepted model of starch granule organization [13], molecular weight of amylopectin and distribution of amylopectin structural units have a great impact on crystallinity of starch granule, determining granule structure and consequently its functional properties. Moreover, JANE and CHEN [14] showed that the amylopectin chain length distribution and amylose molecular size have a great impact on viscosity of starch paste. Molecular weight distribution of amylose and amylopectin molecules together with amylopectin side chain length distribution in starch from various wheat cultivars were extensively studied [15–19].

On the other hand, although the composition and contents of essential nutrients of spelt grain are widely documented, little or no data regarding the structure and polysaccharide composition of spelt starch granules are available in scientific literature. Therefore, we decided to study molecular and selected physicochemical properties of spelt and wheat starches isolated from spelt and flour commercially available on Polish market. For each starch studied, following properties were examined: molecular weight ( $M_w$ ) and radii of gyration ( $R_g$ ) of starch polysaccharide chains, distribution of amylopectin structural units, crystallinity, thermal properties, pasting viscosity profiles, susceptibility to  $\alpha$ -amylolysis, swelling power and solubility.

## MATERIALS AND METHODS

### Starch isolation

Spelt and wheat starches were isolated from spelt (Biopont, Budapest, Hungary) and wheat (Polskie Zakłady Zbozowe, Krakow, Poland) flour, respectively, by previously described methods [20].

### Determination of molecular weight and radii of gyration of starch polysaccharide molecules by HPSEC-MALLS-RI

The high-performance size exclusion chromatography (HPSEC) system consisted of a pump (Ultimate 3000, Dionex, Palo Alto, California, USA), an injection valve (model 7021, Rheodyne, Palo Alto, California, USA), a guard column (TSK PWH, Tosoh, Tokyo, Japan) and two connected size exclusion columns TSKgel GMPWXL

(300×7.8 mm, Tosoh) and TSKgel 2500 PWXL (300×7.8 mm, Tosoh).

A multiangle laser light scattering (MALLS) detector (Dawn-DSP-F, Wyatt Technology, Santa Barbara, California, USA) and a differential refractive index (RI) detector (model SE71, Shodex, Tokyo, Japan) were connected to the columns. The columns were maintained at 40 °C and the RI detector at 35 °C. The mobile phase (0.15 mol·l<sup>-1</sup> NaNO<sub>3</sub> with sodium azide) was filtered through 0.2 μm and 0.1 μm cellulose acetate filters (Whatman, Maidstone, United Kingdom). The flow rate of the mobile phase and the sample injection volume were 0.4 mol·min<sup>-1</sup> and 500 μl, respectively. The output voltage of RI and light scattering (LS) at 18 angles was used for calculation of the weight-average  $M_w$  and  $R_g$  using Astra 4.70 software (Wyatt Technology). A Berry plot with third-order polynomial fit was applied for the calculation of  $M_w$  and  $R_g$  values [21–23].

### HPSEC-MALLS-RI data analysis

The theory and principle of MALLS is described in the literature [21]. The eluate from the HPSEC column was measured in narrow increments, slice by slice, by the MALLS and RI detector. For each slice of the elution pattern, corresponding to one elution volume ( $V_i$ ), concentration ( $c_i$ ) was calculated from the differential refractive index response. Following this determination, the measurement of the light scattered using the 18 Dawn-DSP photodiodes allowed the determination of molecular weight ( $M_{wi}$ ) and radius of gyration  $R_{gi}$  of the polymer based on the following equation:

$$\frac{R_\theta}{K^*c_i} = M_{wi} - \frac{16\pi^2}{3\lambda^2 R_{gi}^2 M_{wi} \sin^2(\theta/2)} \quad (1)$$

where  $R_\theta$  is the excess Rayleigh ratio of the solute under angle  $\theta$ ,  $K^*$  is instrumental optical constant and  $\lambda$  is the wavelength of the incident laser beam.

$R_\theta$  was defined by equation:

$$R_\theta = f(I_s/I_0) \quad (2)$$

where  $f$  is geometrical constant,  $I_s$  is intensity of scattered light and  $I_0$  is intensity of incident light.

Instrumental constant  $K^*$  could be calculated from the following equation:

$$K^* = \frac{4\pi^2 n_0^2 (dn/dc)^2}{\lambda^4 N_A} \quad (3)$$

where  $n_0$  is the index of refraction of the solvent,  $N_A$  is Avogadro's number,  $dn/dc$  is the differential refractive index increment of the polymer.

The MALLS data were evaluated through a Debye plot, depicting a function of the excess

Rayleigh scattering against  $\sin^2(\theta/2)$ .  $M_w$  and  $R_g$  were obtained from the intercept and slope, respectively, of the Debye plot extrapolated to  $0^\circ$ . In our case the Debye plot for eluted polysaccharides was expressed by the Berry method ( $\sqrt{(K^*c/R)}$  vs  $\sin^2(\theta/2)$ ) using a 3rd order polynomial fit to take care of a curvature at the low angles.

#### Sample preparation for HPSEC

Starch (1 g) moistened with water (10 ml) was suspended in dimethylsulphoxide (DMSO, 90 ml) and boiled for 2 h with agitation. Then, the starch solution was agitated for 24 h at  $25^\circ\text{C}$ , followed by precipitation of starch with ethanol (500 ml). The precipitate was centrifuged (41.6 Hz, 20 min), washed three times with ethanol and dried overnight under vacuum at room temperature. The purified starch (30 mg) was suspended in 1 ml of  $0.15 \text{ mol}\cdot\text{l}^{-1}$   $\text{NaNO}_3$  in 10 ml measuring flask. Starch suspension was slowly agitated by magnetic stirrer and 6 ml of DMSO was gradually added to the suspension. Temperature of the suspension was then increased to  $80^\circ\text{C}$  and the suspension was kept at this temperature, slowly mixed, until complete dissolution of starch polysaccharide chains was obtained. Clear solution was cooled to  $25^\circ\text{C}$  and DMSO was added to the measuring flask in order to obtain final volume of 10 ml.

Prior to HPSEC injection, the solution was filtered through a filter (pore size  $0.8 \mu\text{m}$ ; Whatman).

#### Determination of amylopectin chain length distribution

Starch sample (20 mg) was suspended in water (6.5 ml) and heated for 30 min at  $95^\circ\text{C}$ . After cooling down, the starch solution was diluted with water (2.5 ml) and acetate buffer (pH 3.5, 1 ml). An aliquot of the stock solution of *Pseudomonas amyloclavata* isoamylase (glycogen 6-glucohydrolase EC.3.2.1.68; Sigma, Poznan, Poland) in acetate buffer (pH 3.5,  $0.100 \text{ cm}^3$ ,  $54000 \text{ U}\cdot\text{ml}^{-1}$ ) was added and the solution was incubated for 24 h at room temperature.

For a portion of the digest (2 ml), pH was increased to 4.8 with acetate buffer (0.5 ml, pH 4.8) followed by addition of  $\beta$ -amylase (20 mg,  $29 \text{ U}\cdot\text{mg}^{-1}$ ). Incubation was completed after 24 h by bringing the samples to boiling.

#### Unit chain distribution

High performance size exclusion chromatography was performed using HPSEC-MALLS-RI system. Flow rate of the solvent ( $0.15 \text{ mol}\cdot\text{l}^{-1}$   $\text{NaNO}_3$ ) was  $0.40 \text{ ml}\cdot\text{min}^{-1}$  and injected volume was  $0.1000 \text{ ml}$ .

#### X-ray diffractometry

X-ray powder diffractometry was performed according to GERARD et al. [24]. Samples of spelt and wheat starches were adjusted to  $200 \text{ g}\cdot\text{kg}^{-1}$  water content. Equilibrated samples were sealed between two tape foils to maintain a stable water content throughout the measurement. Diffraction diagrams were recorded using X'pert-type Phillips diffractometer (Phillips, Groeningen, The Netherlands) with a cobalt lamp of  $\lambda = 1.78896 \text{ \AA}$  (30 mA and 40 kV) and in a scanning region of  $2\theta$  from  $5^\circ$  to  $60^\circ$  in  $0.02^\circ$  intervals.

#### Susceptibility to $\alpha$ -amylolysis

$\alpha$ -Amylase from porcine pancreas (EC.3.2.1.1; Merck, Darmstadt, Germany) was reconstituted in  $20 \text{ mmol}\cdot\text{l}^{-1}$  phosphate buffer (pH 6.5–7.0) containing  $2 \text{ mmol}\cdot\text{l}^{-1}$   $\text{NaCl}$  and  $0.25 \text{ mmol}\cdot\text{l}^{-1}$   $\text{CaCl}_2$  to obtain a stock solution with an enzyme activity of  $250 \text{ U}\cdot\text{ml}^{-1}$ .

Native starch samples were precisely weighed into Erlenmeyer flasks and suspended in the phosphate buffer (38 ml). Aliquots of the enzyme stock solution (2 ml) were added to achieve a  $1 \text{ mg}\cdot\text{ml}^{-1}$  final concentration of starch and a final enzyme activity of  $12.5 \text{ U}\cdot\text{mg}^{-1}$  substrate. The Erlenmeyer flasks were incubated at  $37^\circ\text{C}$ . Aliquots (2 ml) were collected within different time intervals. The amount of solubilized starch was determined by the 3,5-dinitrosalicylic acid method [24]. Amylolysis was performed at  $37^\circ\text{C}$  for 750 min. The extent of starch amylolysis was calculated as the ratio of the amounts of hydrolysed starch and total dry substrate.

The  $(1/c)$  versus time linear relationship for subsequent stages of the enzymatic reaction was plotted using linear regression method ( $R = 0.97\text{--}0.99$ ). Slopes of the plotted lines provided rate constants for both stages of the studied reactions.

#### Swelling power and solubility

The swelling power and solubility of starches were determined by the modified method of SUBRAMANIAN et al. [25]. A starch suspension ( $0.15 \text{ g}$  dry weight basis) in water (8 ml) was agitated for 30 min at  $75^\circ\text{C}$ . Subsequently, it was immersed in an ice bath for 1 min, equilibrated at  $25^\circ\text{C}$ , and centrifuged at  $2000 \times g$  for 15 min. The supernatant was transferred to a preweighed dish and dried overnight at  $130^\circ\text{C}$ . The swelling power was calculated as the ratio of the weights of swelled sediment and initial sample, and the solubility was calculated as the percentage of starch dissolved in water.

### Pasting properties

Pasting curves of spelt and wheat starches (6%, w/w) were measured with a Rapid Visco-analyzer (RVA, Newport Scientific, Newport, Australia). The starch suspensions were heated at a rate of  $4.5^{\circ}\text{C}\cdot\text{min}^{-1}$  from  $50^{\circ}\text{C}$  up to  $95^{\circ}\text{C}$ , maintained at this temperature for 10 min, cooled down to  $50^{\circ}\text{C}$  at a rate of  $4.5^{\circ}\text{C}\cdot\text{min}^{-1}$ , and held for 10 min.

### Thermal properties

Differential scanning calorimetry (DSC) experiments were performed in Mettler-Toledo 821e calorimeter (Mettler – Toledo, Greifensee, Switzerland) equipped with an intracooler Haake (Haake, Vreden, Germany) in  $40\ \mu\text{l}$  aluminium crucibles under constant flow of argon ( $80\ \text{ml}\cdot\text{min}^{-1}$ ) in a temperature range of  $25$ – $125^{\circ}\text{C}$ . Starch ( $1.5$ – $2.0\ \text{mg}$ ) was sealed in an aluminium pan with water in a ratio of  $1:4$  (starch/water, w/w ratio). Pans were sealed and kept for 1 h at room temperature before heating in DSC. An empty pan was used as reference.

## RESULTS AND DISCUSSION

### Molecular weight and radii of gyration distribution

Superimposed chromatograms of wheat starch taken with RI detector and LS detector diode at a  $90^{\circ}$  angle, are given in Fig. 1. Based on the pattern, the peak was arbitrarily divided into three regions attributed to amylopectin, intermediate and amylose fractions. Chromatograms of spelt starch resembled those of the wheat starch. Therefore, the same approach was applied for all samples.  $M_w$  and  $R_g$  values were calculated for the whole complex peak of the eluate and for each of its regions.

$M_w$ ,  $R_g$  and polydispersity index (*PDI*) values for spelt and wheat samples are given in Tab. 1. It can be clearly seen that polysaccharide chains from wheat starch exhibited higher values  $M_w$  and

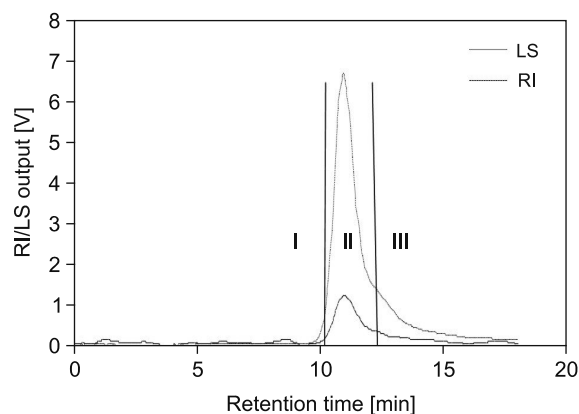


**Fig. 1.** Superimposed chromatograms of RI and LS at  $90^{\circ}$  detector outputs for spelt starch eluted from size exclusion columns.

Regions I, II and III were established for amylopectin, intermediate and amylose fractions, respectively.

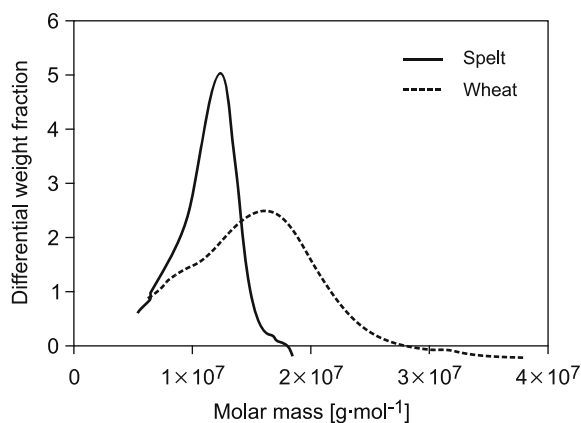


**Fig. 2.** Plots of differential weight fraction versus elution volume for spelt and wheat starches.

$R_g$  than spelt polysaccharide chains for all regions established in the chromatogram. Data from both RI and LS detectors facilitated calculations of differential molar mass distribution with the Astra 4.73.04 software. Plot of differential weight fraction versus elution volume for both starches

**Tab. 1.** Characteristics of spelt and wheat starch polysaccharides.

	Spelt			Wheat		
	$M_w$ [ $\text{g}\cdot\text{mol}^{-1}$ ]	<i>PDI</i>	$R_g$ [nm]	$M_w$ [ $\text{g}\cdot\text{mol}^{-1}$ ]	<i>PDI</i>	$R_g$ [nm]
Whole peak	$(0.829 \pm 0.24) \times 10^7$	1.820		$(2.307 \pm 0.35) \times 10^7$	2.150	
Fraction I	$(2.078 \pm 0.15) \times 10^7$	1.251	$101.0 \pm 3.4$	$(3.953 \pm 0.17) \times 10^7$	1.510	$82.0 \pm 4.8$
Fraction II	$(0.893 \pm 0.37) \times 10^7$	1.120	$61.1 \pm 5.1$	$(2.074 \pm 0.40) \times 10^7$	1.210	$74.2 \pm 4.7$
Fraction III	$(0.433 \pm 0.17) \times 10^7$	1.085	$77.1 \pm 3.5$	$(1.795 \pm 0.4) \times 10^7$	1.162	$83.2 \pm 3.2$

Values are mean of three independent experiments  $\pm$  standard deviation.

$M_w$  – molecular weight, *PDI* – polydispersity index ( $PDI = M_w/M_n$ , where  $M_n$  is number average molecular weight),  $R_g$  – radius of gyration.

**Tab. 2.** Characteristics of amylopectin structural units of spelt and wheat amylopectin chains.

	Spelt				Wheat			
	$M_w$ [g·mol <sup>-1</sup> ]	<i>PDI</i>	$R_g$ [nm]	<i>m</i> [%]	$M_w$ [g·mol <sup>-1</sup> ]	<i>PDI</i>	$R_g$ [nm]	<i>m</i> [%]
Fraction I	$(3.546 \pm 0.15) \times 10^5$	1.506	$46.7 \pm 3.5$	0.4	$(1.691 \pm 0.25) \times 10^5$	1.800	$63.3 \pm 4.0$	28.9
Fraction II	$(6.808 \pm 0.12) \times 10^3$	1.096	$90.5 \pm 4.2$	11.4	$(17.35 \pm 0.10) \times 10^3$	1.020	$95.6 \pm 2.5$	9.7
Fraction III	nd	nd	nd	nd	$(8.214 \pm 0.40) \times 10^3$	1.064	$118.4 \pm 4.1$	28.8
Fraction IV	$(3.418 \pm 0.35) \times 10^3$	1.730	$65.4 \pm 3.0$	88.2	$(5.277 \pm 0.22) \times 10^3$	1.005	$88.2 \pm 2.5$	32.8

Mean of three independent experiments  $\pm$  standard deviation.

$M_w$  – molecular weight, *PDI* – polydispersity index ( $PDI = M_w/M_n$ , where  $M_n$  is number average molecular weight),  $R_g$  – radius of gyration, *m* – mass ratio, nd – not detected.

studied is shown in Fig. 2. Wheat starch polysaccharides exhibited much broader molecular weight distribution than polysaccharide chains originating from spelt starch. Values of *PDI* calculated for whole eluted peak and for each region also supported this observation.×

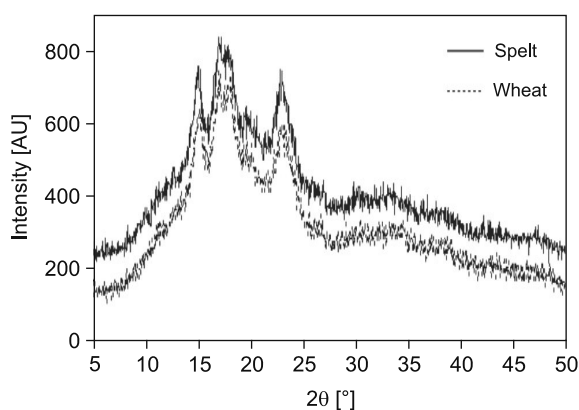
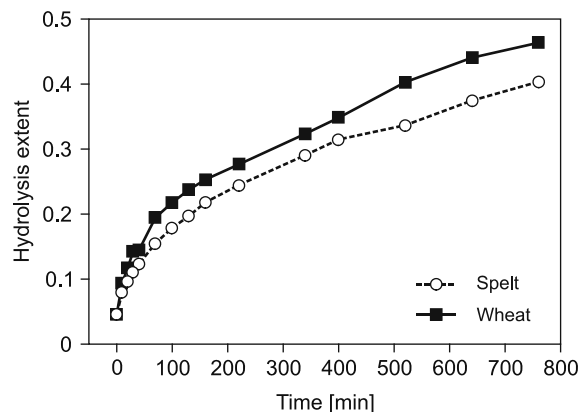
#### Amylopectin chain length distribution

Chromatograms of the isoamylase-debranched amylopectin chains for spelt and wheat starches were divided arbitrarily into four fractions based on the shape of traces of both detectors (LS and RI). Average  $M_w$ ,  $R_g$  and mass ratio of eluted molecules belonging to each peak were calculated (Tab. 2). According to HIZUKURI [26, 27], chains eluted in fraction IV could be classified as smallest A-type chains, whereas Fractions III and Fraction II represented  $B_1$  chains and larger B chains ( $B_{\geq 2}$ ), respectively. Molecules eluted in Fraction I could be regarded as amylose chains. Surprisingly, the presented data showed that, in the case of spelt starch, majority of amylopectin structural units consisted of the smallest A-type chains. Mass ratio of such chains was found to be twice as

high as the mass ratio of A-type chains obtained for wheat amylopectin. Values of  $M_w$  and  $R_g$  of spelt amylopectin A and  $B_{\geq 2}$  chains were significantly lower as compared with respective values of molecular moments of the same type chains found for wheat amylopectin. It is worthy of note that  $B_1$  chains were not detectable by HPSEC of debranched spelt amylopectin chains.

#### X-ray diffractometry

X-ray diffractograms of wheat and spelt starches showed a typical A-type pattern of cereal starch (Fig. 3). The starches showed strong reflections at  $2\theta = 15^\circ, 17^\circ, 18^\circ,$  and  $23^\circ$ . Intensity of the peaks on the spelt starch diffractogram was higher as compared with intensity of peaks recorded for wheat starch, suggesting higher crystallinity of spelt starch granule. On the diffractograms of both starches, additional peak at  $2\theta = 20^\circ$  was observed, indicating presence of crystalline V-type amylose-lipid complexes [18]. The intensity of amylose-lipid peak was observed to be higher in spelt starch than in wheat starch.

**Fig. 3.** X-ray diffraction patterns of spelt and wheat starches.**Fig. 4.** Course of enzymatic hydrolysis of spelt and wheat starches.

**Tab. 3.** Rate constants of  $\alpha$ -amylolysis of spelt and wheat starches.

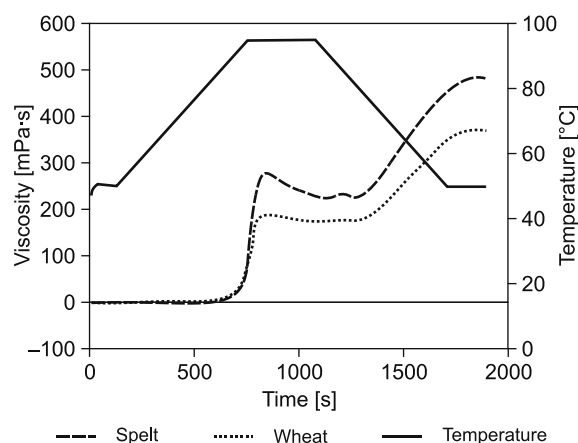
	Spelt	Wheat
$k_1$ [mg·ml <sup>-1</sup> ·min <sup>-1</sup> ]	$(2.3 \pm 0.1) \times 10^{-3}$	$(3.5 \pm 0.1) \times 10^{-3}$
$k_2$ [mg·ml <sup>-1</sup> ·min <sup>-1</sup> ]	$(4.5 \pm 0.2) \times 10^{-4}$	$(4.6 \pm 0.1) \times 10^{-4}$

Mean of three independent experiments  $\pm$  standard deviation.

**Tab. 4.** Swelling power, solubility and pasting properties of spelt and wheat starches.

	Spelt	Wheat
Swelling power [g·g <sup>-1</sup> ]	$6.64 \pm 0.2$	$7.20 \pm 0.3$
Solubility [%]	$1.6 \pm 0.1$	$2.3 \pm 0.1$
Pasting temperature [°C]	$87.7 \pm 0.58$	$86.2 \pm 0.58$
Peak viscosity [mPa s]	$280 \pm 3.21$	$192 \pm 3.21$
Trough viscosity [mPa s]	$235 \pm 3.46$	$170 \pm 1.73$
Breakdown viscosity [mPa s]	$45 \pm 1.23$	$22 \pm 1.13$
Final viscosity [mPa s]	$496 \pm 2.83$	$360 \pm 3.53$

Mean of three independent experiments  $\pm$  standard deviation.

**Fig. 5.** Pasting profiles of spelt and wheat starches.

### Susceptibility to $\alpha$ -amylolysis

The course enzymatic hydrolysis of wheat and spelt starch samples is presented in Fig. 4. A classical two-stage hydrolysis was observed for both starches. Rate constants as calculated for each of the two stages of enzymatic hydrolysis, together with the final extent of reaction for wheat and spelt starches, are presented in Tab. 3. Due to the much lower rate constant for the first stage of hydrolysis and the lower final extent of reaction, spelt starch could be regarded as less susceptible to  $\alpha$ -amylolysis than wheat starch. Granule size [28], crys-

talline organization [29], amylose/amylopectin ratio [30], and the possibility of the formation of lipid-amylose complexes [31, 32] are the main factors influencing susceptibility of granular starches to amylolysis. Susceptibility of cereal starches exhibiting A-type crystallinity to  $\alpha$ -amylolysis is much higher than that of tuber starches with B-type crystallinity. Amylopectin molecules of the A-granule starch consist of more long chains but less short chains, while those of B-granule starch consist of more short chains but less long chains. Therefore, one could assume that the lower susceptibility of the spelt starch granules to  $\alpha$ -amylolysis could be related to the higher number of small chains constituting spelt amylopectin, together with formation of stronger amylose lipid, as compared with wheat starch.

### Swelling power and solubility

Swelling power and solubility of spelt and wheat starches are given in Tab. 4. Spelt starch showed slightly lower, though statistically significant, values of both swelling power and solubility than wheat starch. Swelling power and solubility could be used, to some extent, as a measure of the magnitude of interaction between starch chains within amorphous and crystalline domains. Swelling power and solubility of starches could be affected by the amylose/amylopectin ratio, amylopectin degree of branching and by the length of amylopectin side chains. Formation of strong amylose lipid complexes have a restricting impact on swelling and solubility. Therefore, lower swelling power and solubility of spelt starch could be attributed to the formation of a stronger amylose lipid complex and to higher crystallinity degree of spelt starch granules than in wheat starch.

### Pasting properties

The RVA amylograms of spelt and wheat starches are presented in Fig. 5 and pasting properties are given in Tab. 4. All pasting parameters derived from spelt starch amylograms were found to be significantly higher than the respective values obtained for wheat starch. The pasting properties of starches, characterized by amylograms, seem to be related to complex factors as amylose content, branching architecture of amylopectin, ratio of amylose/amylopectin, and the presence of lipids that can form a complex with amylose [33]. On the other hand, SHIBANUMA et al. [34] suggests that the molecular structure of amylose and amylopectin appears to be the main factor influencing pasting properties of starches. TAKEDA et al. [35] showed that starches with high molecular weight amylose and amylopectins con-

tained a lower amount of long branch chains as well as lower degree of branching in amylopectins, which resulted in an increase in the peak viscosity and breakdown, while decreasing the setback and final viscosity. Spelt starch amylopectin side chains contained much more short chains than wheat starch amylopectin structural units. Additionally, X-ray data indicated that amylose/lipid complexes formed in spelt starch are stronger than complexes formed in wheat starch. This could explain the fact that spelt starch pasting parameters were higher than the corresponding pasting parameters of wheat starch.

### Thermal properties

Thermograms of spelt and wheat starches are presented in Fig. 6. Tab. 5 gives the onset ( $T_o$ ), peak ( $T_p$ ), conclusion ( $T_c$ ) and transition enthalpy ( $\Delta H$ ) for melting of spelt and wheat starches. No significant differences between melting temperatures and melting enthalpies for spelt and wheat starches were found. These findings correspond well with already published data regarding thermal properties of several spelt cultivars [36].

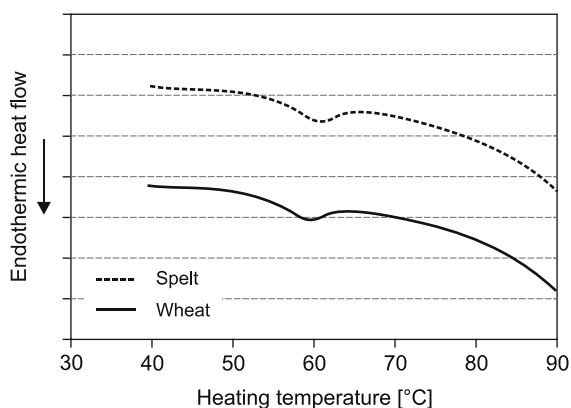


Fig. 6. Thermograms of spelt and wheat starches

Tab. 5. Thermal properties of spelt and wheat starches.

	Spelt	Wheat
$T_o$ [°C]	56.79 ± 0.91	54.71 ± 0.78
$T_p$ [°C]	61.00 ± 0.47	59.46 ± 0.63
$T_c$ [°C]	65.07 ± 0.85	63.19 ± 1.23
$\Delta H$ [J·g <sup>-1</sup> ]	8.11 ± 0.55	6.80 ± 0.79

Mean of three independent experiments ± standard deviation.

$T_o$ ,  $T_p$ ,  $T_c$  – onset, peak and conclusion temperature respectively;  $\Delta H$  – enthalpy change.

### CONCLUSIONS

The present study indicates that molecular structures of spelt and common wheat starch polysaccharide chains are significantly different, with wheat starch polysaccharide molecules exhibiting much higher  $M_w$  values than spelt starch chains. Distribution of amylopectin side chains of spelt starch indicates that spelt amylopectin contains twice as much of the shortest, A-type chains than wheat amylopectin. Results obtained clearly show that spelt and common wheat starches significantly differ from each other, especially in values of molecular moments of polysaccharide chains and in the distribution of amylopectin structural units.

Further research including more spelt varieties is needed to correlate molecular structure of spelt starch polysaccharide molecules with certain physicochemical and functional properties, especially pasting profiles and susceptibility to  $\alpha$ -amylolysis of spelt starch.

### REFERENCES

- Rüegger, A. – Winzeler, H.: Performance of spelt (*Triticum spelta* L.) and wheat (*Triticum aestivum* L.) at two different seeding rates and nitrogen levels under contrasting environmental conditions. *Journal of Agronomy and Crop Science*, 170, 1993, pp. 289–295.
- Kema, G. H. J.: Resistance in spelt wheat to yellow rust. III. Phylogenetical considerations. *Euphytica*, 63, 1992, pp. 225–231.
- Ortiz-Monasterio, I. – Graham, R. D.: Breeding for trace minerals in wheat. *Food and Nutrition Bulletin*, 21, 2000, pp. 392–396.
- Cakmak, I. – Torun, A. – Millet, E. – Feldman, M. – Fahima, T. – Korol, A. – Nevo, E. – Braun, H. J. – Ozkan, H.: *Triticum dicoccoides*: an important genetic resource for increasing zinc and iron concentration in modern cultivated wheat. *Soil Sciences and Plant Nutrition*, 50, 2004, pp. 1047–1054.
- Cakmak, I. – Pfeiffer, W. H. – McClafferty, B.: Biofortification of durum wheat with zinc and iron. *Cereal Chemistry*, 87, 2010, pp. 10–20.
- Gomez-Becerra, H. F. – Erdemb, H. – Yazici, A. – Tutus, Y. – Torun, B. – Ozturk, L. – Cakmak, I.: Grain concentrations of protein and mineral nutrients in a large collection of spelt wheat grown under different environments. *Journal of Cereal Science*, 52, 2010, pp. 342–349.
- Labuschagne, M. T. – Geleta, N. – Osthoff, G.: The influence of environment on starch content and amylose to amylopectin ratio in wheat. *Starch/Stärke*, 59, 2007, pp. 234–238.
- Tako, M. – Hizukuri, S.: Rheological properties of

- wheat (Halberd) amylopectin. *Starch/Stärke*, 55, 2003, pp. 345–349.
9. Jane, J. L.: Structure of starch granules. *Journal of Applied Glycoscience*, 54, 2007, pp. 31–36.
  10. Jane, J. – Chen, Y. Y. – Lee, L. F. – McPherson, A. E. – Wong, K. S. – Radosavljevic, M. – Kasemsuwan, T.: Effects of amylopectin branch chain length and amylose content on the gelatinization and pasting properties of starch. *Cereal Chemistry*, 76, 1999, pp. 629–637.
  11. Singh, N. – Isono, N. – Srichuwong, S. – Noda, T. – Nishinari, K.: Structural and viscoelastic properties of potato starches. *Food Hydrocolloid*, 22, 2008, pp. 979–988.
  12. Singh, N. – Singh, S. – Isono, N. – Noda, T. – Singh, A. M.: Diversity in amylopectin structure, thermal and pasting properties of starches from wheat varieties/lines. *International Journal of Biological Macromolecules*, 45, 2009, pp. 298–304.
  13. Gallant, J. G. – Bouchet, B. – Baldwin, M.: Microscopy of starch: Evidence of a new level of granule organization. *Carbohydrate Polymers*, 32, 1997, pp. 177–191.
  14. Jane, J. L. – Chen, Y. Y.: Effects of amylose molecular size and amylopectin branch chain length on paste properties of starch. *Cereal Chemistry*, 69, 1992, pp. 60–65.
  15. Bechtel, D. B. – Zayas, I. – Dempster, R. – Wilson, J. D.: Size distribution of starch granules isolated from hard red winter wheat and soft red winter wheat. *Cereal Chemistry*, 70, 1993, pp. 238–240.
  16. You, S. – Fiedorowicz, M. – Lim, S. T.: Molecular characterization of wheat amylopectins by multiangle laser light scattering analysis. *Cereal Chemistry*, 76, 1999, pp. 116–121.
  17. Jane, J. – Chen, Y. Y. – Lee, L. F. – McPherson, A. E. – Wong, K. S. – Radosavljevic, M. – Kasemsuwan, T.: Effects of amylopectin branch chain length and amylose content on the gelatinization and pasting properties of starch. *Cereal Chemistry*, 76, 1999, pp. 629–637.
  18. Singh, S. – Singh, N. – Isono, N. – Noda, T.: Relationship of granule size distribution and amylopectin structure with pasting, thermal, and retrogradation properties in wheat starch. *Journal of Agricultural and Food Chemistry*, 58, 2010, pp. 1180–1188.
  19. Singh, N. – Singh, S. – Isono, N. – Noda, T. – Singh, A. M.: Diversity in amylopectin structure, thermal and pasting properties of starches from wheat varieties/lines. *International Journal of Biological Macromolecules*, 45, 2009, pp. 298–304.
  20. Richter, M. – Augustat, S. – Schierbaum, F.: *Ausgewählte Methoden der Stärkechemie*. Leipzig: VEB Fachbuchverlag, 1968. 254 pp.
  21. Aberle, Th. – Burchard, W. – Vorweg, W. – Radosta, S.: Conformational contribution of amylose and amylopectin to the structural properties of starches from various sources. *Starch/Stärke*, 46, 1994, pp. 329–336.
  22. Hanselmann, R. – Burchard, W. – Ehrat, M. – Widmer, H. M.: Structural properties of fractionated starch polymers and their dependence on the dissolution process. *Macromolecules*, 29, 1996, pp. 3277–3282.
  23. Bello-Perez, L. A. – Paredes-Lopez, O. – Roger, P. – Colonna, P.: Molecular characterization of some amylopectins. *Cereal Chemistry*, 73, 1996, pp. 12–17.
  24. Gerard, C. – Colonna, P. – Buleon, A. – Planchot, V.: Amylolysis of maize mutant starches. *Journal of the Science of Food and Agriculture*, 81, 2001, pp. 1281–1287.
  25. Subramanian, V. – Hosoney, R. C. – Bramel-Cox, P.: Shear thinning properties of sorghum and corn starches. *Cereal Chemistry*, 71, 1994, pp. 272–275.
  26. Hizukuri, S.: Relationship between diastribution of the chain length of amylopectin and the crystalline structure of starch granules. *Carbohydrate Research*, 141, 1985, pp. 295–306.
  27. Hizukuri, S.: Polymodal distribution of the chain length distribution of amylopectin and its significance. *Carbohydrate Research*, 147, 1986, pp. 342–347.
  28. Ring, S. G. – Gee, J. M. – Whittam, M. – Orford, P. – Johnson, I. T.: Resistant starch: Its chemical form in foodstuffs and digestibility in vitro. *Food Chemistry*, 28, 1988, pp. 97–109.
  29. Gallant, D. J. – Bouchet, B. – Bouleon, A. – Perez, S.: Physical properties of starch granules and susceptibility to enzymatic degradation. *European Journal of Clinical Nutrition*, 46, 1992, pp. 3–16.
  30. Snow, P. – O’Dea, K.: Factors affecting the rate of hydrolysis of starch in food. *The American Journal of Clinical Nutrition*, 34, 1981, pp. 2721–2727.
  31. Larsson, K. – Miezi, Y.: On the possibility of dietary fiber formation by interaction in the intestine between starch and lipids. *Starch/Stärke*, 31, 1979, pp. 301–301.
  32. Holm, O. – Bjorck, I. – Ostrowska, S. – Eliasson, E. C. – Asp, N. G., – Larsson, K., – Lundquist, I.: Digestibility of lipid-amylose complexes in vitro and in vivo. *Starch/Stärke*, 35, 1983, pp. 294–296.
  33. Tester, R. F. – Morrison, W. R.: Swelling and gelatinization of cereal starches. II. Waxy rice starches. *Cereal Chemistry*, 67, 1990, pp. 551–557.
  34. Shibamura, Y. – Takeda, Y. – Hizukuri, S.: Molecular and pasting properties of some wheat starches. *Carbohydrate Polymers*, 29, 1996, pp. 253–261.
  35. Takeda, Y. – Takeda, C. – Suzuki, A. – Hizukuri, S.: Structure and properties of sago starches with low and high viscosities on amylograph. *Journal of Food Science*, 54, 1989, pp. 177–182.
  36. Wilson, J. D. – Bechtel, D. B. – Wilson, G. W. T. – Seib, P. A.: Bread quality of spelt wheat and its starch. *Cereal Chemistry*, 8, 2008, pp. 629–638.

Received 5 April 2013; 1st revised 10 June 2013; 2nd revised 19 July 2013; accepted 31 July 2013; published online 3 February 2014.